Vacancy clustering and diffusion in silicon: Kinetic lattice Monte Carlo simulations

Benjamin P. Haley

Department of Applied Science, University of California, Davis, California 95616, USA

Keith M. Beardmore

MZA Associates, Albuquerque, New Mexico 87106, USA

Niels Grønbech-Jensen

Department of Applied Science, University of California, Davis, California 95616, USA

Diffusion and clustering of lattice vacancies in silicon as a function of temperature, concentration, and interaction range are investigated by kinetic lattice Monte Carlo simulations. It is found that higher temperatures lead to larger clusters with shorter lifetimes on average, which grow by attracting free vacancies, while clusters at lower temperatures grow by the aggregation of smaller clusters. Long interaction ranges produce enhanced diffusivity and fewer clusters. Greater vacancy concentrations lead to more clusters, with fewer free vacancies, but the size of the clusters is largely independent of concentration. Vacancy diffusivity is shown to obey power law behavior over time, and the exponent of this law is shown to increase with concentration, at fixed temperature, and decrease with temperature, at a fixed concentration.

PACS number(s): 66.30.Jt

I. INTRODUCTION

The introduction of dopants into crystalline silicon via ion implantation creates damage to the crystal lattice. Lower energy implants, in the 10–100 keV range, create lattice vacancies and interstitial defects which mostly recombine during annealing so that only the implanted ions remain as defects in the lattice.[1] High energy ion implantation, in the MeV range, produces greater physical distance between regions of vacancies and interstitials, so that less recombination occurs. Thus a vacancy layer forms near the surface, and an interstitial layer forms deeper in the silicon. The enhanced diffusion[2,3] of other defects, such as Sb, after high energy Si implants, demonstrates the existence of the vacancy layer near the surface.

Vacancies near the surface of silicon can be used to control the diffusion of subsequently implanted dopants, such as boron, which are sensitive to transient enhanced diffusion. Excess interstitials created by boron implants recombine with vacancies created by previous high energy Si implants, limiting diffusion of the boron dopants.[4] The experimental observations[2,3] of the vacancy layer persist after annealing, indicating the formation of large stable clusters of vacancies. Exploring the mechanisms by which these voids form is important for understanding the implantation and diffusion of dopants in silicon after, e.g., high energy Si implants.

Several theoretical descriptions of the void formation process in silicon exist. General models of Ostwald ripening,[5] the growth of large clusters at the expense of smaller clusters, simulate the dissociation of smaller clusters and the absorption of their constituents into larger clusters.[6] Bongiorno and Columbo[7] used the Stillinger-Weber[8] potential and molecular dynamics simulations to demonstrate that strain fields due to the distortion in the silicon lattice near vacancies affect the capture radius in different directions from a vacancy cluster. Staab *et al.*[9] performed *ab initio* calculations on clusters containing up to 17 vacancies and found that those clusters which form closed rings, for example, those with 6 and 10 vacancies, are exceptionally stable. La Magna *et al.*[10] used lattice Monte Carlo simulations to study the formation of vacancy clusters. They considered various interactions, including an Ising-like binding model in which only nearest neighbor interactions were considered, at 900 °C and a high vacancy concentration of 10^{20} cm^{-3}. They found that a large number of very stable clusters of 6, 10, and 14 vacancies formed. They also used an extended Ising-like model which accounted for second nearest neighbor interactions. This extended binding model did not produce large numbers of the stable clusters of the nearest neighbor model; the extended model resulted in fewer, larger clusters and small clusters were observed to move through the lattice to form larger clusters, in a self-organizing manner. Chakravarthi and Dunham[11] used a rate equation model to study vacancy cluster growth in silicon during a 10 min anneal. They also observed a high incidence of the stable ring clusters with 6, 10, and 14 vacancies. They found that at a lower temperature, 750 °C, smaller clusters with fewer than 36 vacancies were most prominent, while at higher temperature, 950 °C, larger clusters dominated. Prasad and Sinno used molecular dynamics[12] to model the energetics of vacancy cluster formation and used this information to develop a mean-field continuum model[13] of cluster aggregation which also demonstrated the importance of small cluster diffusion in void formation.

Continuum models such as those of Chakravarthi and Dunham[11] and Prasad and Sinno[12,13] must assume the behavior of small vacancy clusters in silicon with respect to how they aggregate, i.e., whether they diffuse or dissociate. Variation in behavior over ranges of temperature or concentration is not considered in these models. Kinetic lattice Monte Carlo (KLMC) models do not make any assumptions regarding the behavior of clusters since they are based on interactions between individual defects. These models can also simulate much larger systems and longer times than molecu-
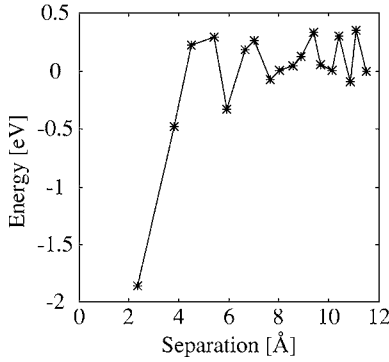
FIG. 1. Vacancy pair interaction energies.

lar dynamics simulations, and can include arbitrarily long range interactions. This work investigates, through a KLMC model, the formation of vacancy clusters and the mechanisms by which clusters grow, as a function of temperature, in Sec. III A, concentration, in Sec. III B, and interaction range, in Sec. III C. The time dependence of diffusivity, D, as a power law of the form,

$$D(t) \sim t^{-\gamma} \tag{1}$$

is studied in each section.

II. SIMULATION METHOD

A. Kinetic lattice Monte Carlo

A Kinetic lattice Monte Carlo method is used to simulate atomic scale diffusion processes. Lattice defects are probed, in random order, and, if a move to a neighbor site is allowed, each defect is moved, one at a time. Defects can include dopants and native point defects, but are limited to vacancies in this work. Possible movements, therefore, include vacancies exchanging lattice sites with lattice atoms or other vacancies. We use the Metropolis[14] algorithm with detailed balance to determine whether a new configuration is accepted. If the move does not lower the system energy, it is accepted, with probability $e^{-\Delta E/2k_BT}$, where k_B is Boltzmann's constant, T is the system temperature, and ΔE is the change in system energy as a result of the move. The system energy in each configuration is the sum of pair interactions between the defects. The values for the pair interactions at given separations on the lattice, out to 18 neighbors, were calculated with *ab initio* methods described in Sec. II B.

The time scale of a KLMC simulation is set by the hopping frequency, ν_H^V, of the vacancies, which is determined by

$$\nu_H^V = \nu_0^V e^{-E_b^V/k_BT}, \tag{2}$$

where ν_0^V is the attempt frequency, and E_b^V is the height of the energy barrier for movement to a nearest neighbor position. In this work, we used ν_0^V calculated with the expression

$$\nu_0^V = \frac{8D_0^V}{a_0^2}, \tag{3}$$

and the values $D_0^V = 1.18 \times 10^{-4}$ cm²/s, and $E_b^V = 0.1$ eV, reported for low density vacancy diffusion by Tang *et al.*,[15] and

a lattice constant of 5.43 Å. This value for E_b^V is less than the 0.2 eV used by other authors,[16,17] but the energy barrier for the diffusion of a single vacancy should be calculated from a known low density system.

After each KLMC step, which randomly visits defects in the system, the simulation time is incremented by the constant time step, which is the exchange time of a vacancy with a Si lattice atom, set by ν_H^V, given by Eq. (2). Updating the system time allows the following definition of a time dependent diffusion coefficient:

$$D^V(t_1, t_2) = \frac{\langle |r_i(t_2) - r_i(t_1)|^2 \rangle_i}{6|t_2 - t_1|}. \tag{4}$$

This definition approaches the thermodynamic diffusion coefficient as $|t_2 - t_1|$ approaches infinity, while also allowing for diffusion studies during various time ranges.

B. *Ab initio* calculations

The pair interactions between vacancies were calculated using the ultrasoft pseudopotential plane wave code VASP,[18] on a 216 atom supercell. The generalized gradient approximation (GGA) was used, along with a 4^3 Monkhorst-Pack[19] **k**-point sampling and a kinetic energy cutoff of 208 eV. All systems were charge neutral. The resulting interaction energies are shown in Fig. 1. In each case a pair of vacancies was placed into the silicon supercell and the initial configuration of atoms was allowed to relax. The final energy of the relaxed configuration was recorded and the process was repeated for all possible shell separations of the vacancy pair out to the cutoff range of 18 shells, the largest separation which could be practically calculated. The final energy at the cutoff range was shifted to zero, so that the interaction vanishes at the cutoff range, and all the other values were shifted by the same amount. These shifted values were recorded as the interaction energies of the vacancy pair. The process of truncating and shifting the energies results in interactions which seem strongly attractive at first and second nearest neighbor positions and weakly repulsive at most larger separations. Thermal fluctuations at elevated temperatures are more likely to overcome the interactions at long range than at short range, making the dissolution of clusters less probable than formation.

The set of interaction energies was incorporated into the KLMC model. For every configuration of vacancies in the KLMC simulations the system energy was calculated as the sum of all the pair interactions between the vacancies in the system, given the shell separation of each vacancy pair, out to the cutoff interaction range. Separate vacancies were not permitted to simultaneously occupy the same lattice site.

III. RESULTS

For each combination of system parameters, five simulations with different random initial distributions of vacancies were performed; the mean results are presented here. Defects were visited randomly at each Monte Carlo step. A defect is a member of a cluster if it is at a nearest neighbor position to at least one other member of the cluster, as in Fig. 2. The
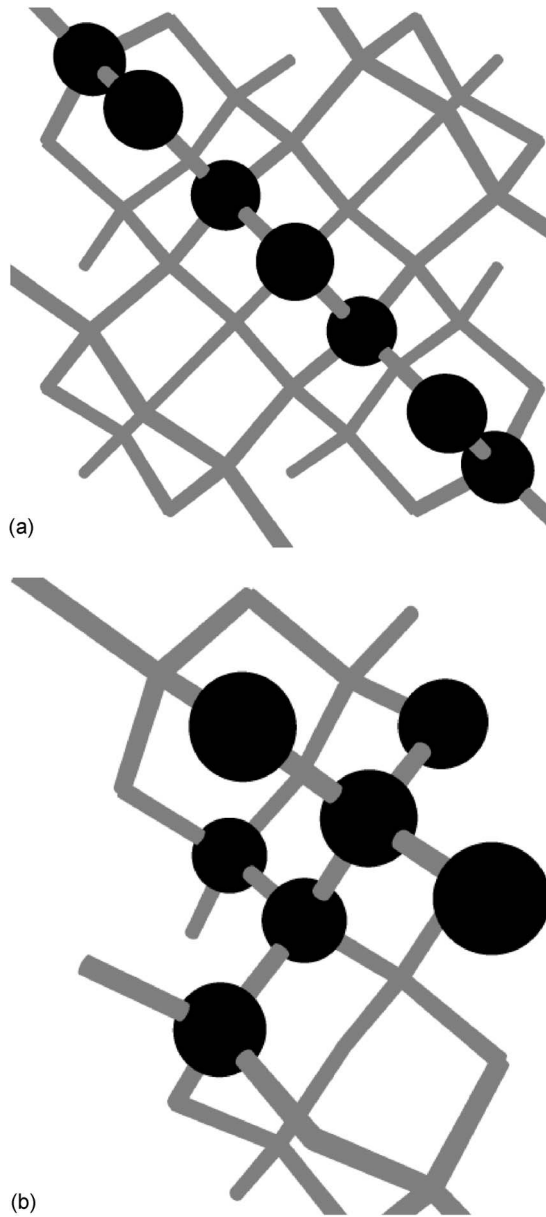
FIG. 3. Vacancy diffusivity at various temperatures, with 10^{18} V cm^{-3} and 18 shell interactions.

greater at lower temperatures. The formation of vacancy clusters over time can be seen in Fig. 4(a). At higher temperatures, fewer clusters form but the number of clusters varies less over time than at lower temperatures. The clusters which form at higher temperatures tend to be larger on average than those formed at lower temperatures, as seen in Fig. 4(b). The change in the number of clusters alone cannot account for the greater size of the clusters formed at higher temperatures. Figure 5 shows the fraction of free vacancies over time for the various temperatures under consideration. During the time interval in which the number of clusters is decreasing and the mean cluster size is growing, in Fig. 4,

FIG. 4. Number of clusters (a) and cluster size (b) at various temperatures, with 10^{18} V cm^{-3} and 18 shell interactions.

FIG. 2. Vacancy clusters on a silicon lattice in a KLMC simulation. Silicon atoms are not shown.

boundary conditions of all simulations were periodic. On all following plots the statistical error is smaller than the symbols used, so error bars are not shown.

A. Temperature

The simulations presented in this section were performed with 170 vacancies in a simulation box 102 unit cells in each dimension, for a vacancy concentration of 10^{18} cm^{-3}. Long range interactions were used, to the 18th nearest neighbor, and the temperature was varied from 700 to 1300 K. Figure 3 shows the diffusivity of vacancies. The period of the initial constant diffusivity, indicating free vacancy diffusion, leads to decreasing diffusivity, as a power law with exponent $\gamma = 0.8 \pm 0.2$, as clusters form. The diffusivity remains greater at higher temperatures, and the power law exponent is
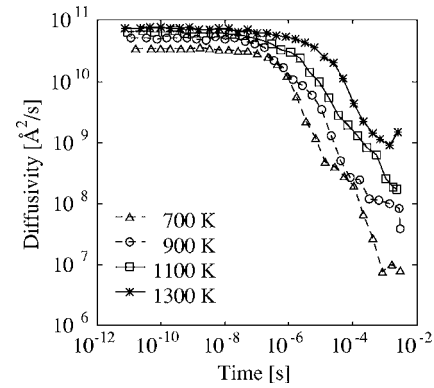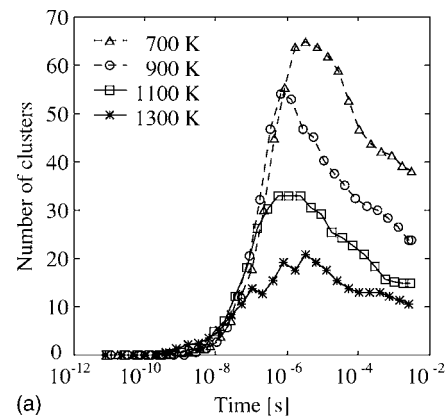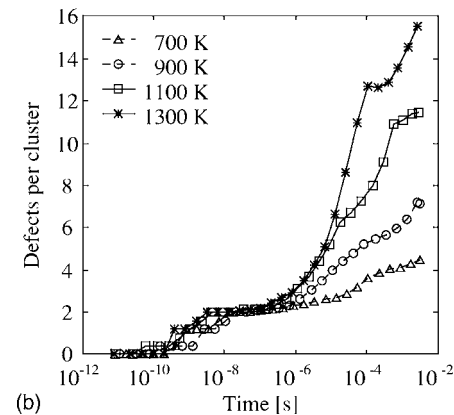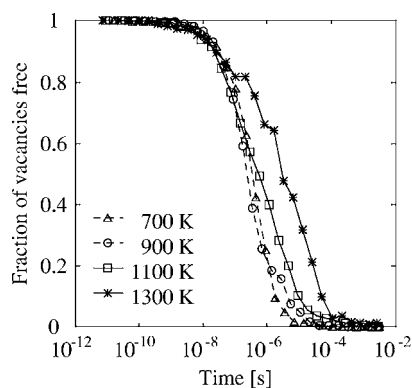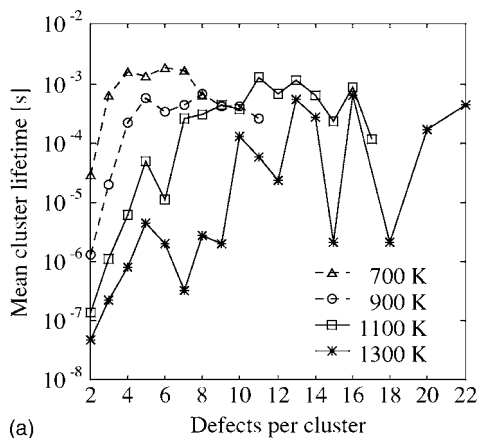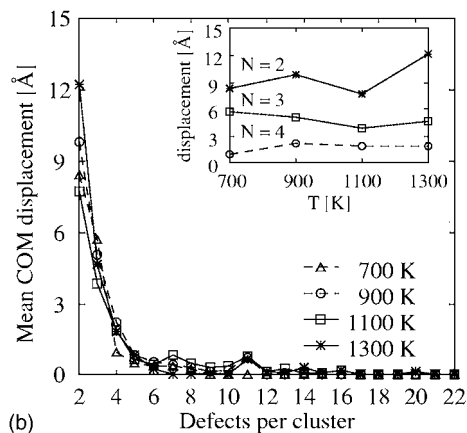
FIG. 5. Fraction of vacancies free at various temperatures, with 10^{18} V cm^{-3} and 18 shell interactions.

more vacancies are likely to be free, not bound in a cluster, at higher temperatures. Thus, while the growth of larger clusters at all temperatures is partly due to the aggregation of smaller clusters and partly due to the capture of free vacancies by existing clusters, the latter effect contributes more at higher temperatures.

The mean lifetime of the clusters, defined for each cluster size as the time over which a cluster consists of that many defects, also depends on temperature. Figure 6(a) shows that

FIG. 6. Mean cluster lifetime (a) and mean displacement of cluster center (b) at various temperatures, with 10^{18} V cm^{-3} and 18 shell interactions.

the lifetime of clusters at lower temperatures is significantly greater than clusters of the same size at higher temperatures. Thermal fluctuations k_BT are larger relative to the vacancy-vacancy binding energy at higher temperatures, increasing the probability that a vacancy will break free from a cluster. Certain cluster sizes have longer mean lifetimes than those with a similar number of vacancies. Clusters with 5, 10, 13, and 16 vacancies exist longer on average than clusters with one more or fewer vacancies, especially at higher temperatures. This trend is similar to the *ab initio* results discussed in Sec. I, which noted stable clusters with 6, 10, and 14 vacancies. It should be noted that the *ab initio* results considered many-body effects while the KLMC results shown here used only pair interactions. Figure 6(b) shows the mean displacement of the cluster center for all cluster sizes observed in the simulations. As expected, the smaller clusters are more mobile on average, but the inset plot shows that the mean displacement of the three smallest clusters, with 2, 3, and 4 vacancies, does not change considerably over the range of temperatures considered.

From the results in Figs. 4–6, the growth of large clusters proceeds by different mechanisms at lower temperatures than at higher temperatures. At lower temperatures, many small clusters, mostly vacancy pairs, form, with most of the vacancies in the system bound in clusters. The pairs remain bound for relatively long times, during which they aggregate into larger clusters. The rate of aggregation is relatively slow because the diffusion of vacancy pairs is slower than the diffusion of free vacancies. At higher temperatures, some vacancy pairs form initially, but many vacancies are still free. The pairs are more likely to dissociate, with the constituent vacancies reforming new pairs. Thus, at higher temperatures the formation of large clusters is a combination of aggregating small clusters and capturing free vacancies. The free vacancies diffuse rapidly so larger clusters can form more quickly at higher temperatures. The continuum models of void growth discussed in Sec. I do not account for this temperature dependence. The difference in the vacancy clustering behavior at lower and higher temperatures can be important if the vacancies are used to control diffusion of other species.

B. Concentration

The simulations presented in this section were performed with a varying number of vacancies in a simulation box 102 unit cells in each dimension, for vacancy concentrations ranging from 10^{17} cm^{-3} to 10^{18} cm^{-3}. Long range interactions were used, to the eighteenth nearest neighbor, and the system temperature was 900 K. Figure 7 shows the vacancy diffusivity over time. For all concentrations considered the vacancies initially diffuse freely. The diffusivity decreases as clusters form, with a power law exponent $\gamma=0.6\pm0.1$, where the higher values correspond to higher concentration. The formation of clusters can be seen in Fig. 8(a). At lower concentrations the number of clusters increases slowly over time, while at higher concentrations a large number of clusters form initially, after which the number of clusters decreases again. Figure 8(b) shows that the clusters, which
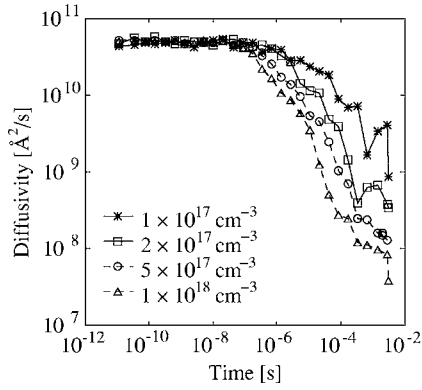
FIG. 7. Vacancy diffusivity at various concentrations, with 18 shell interactions at 900 K.

form initially at all concentrations, tend to be vacancy pairs and that the mean size of the clusters increases at roughly the same rate, with a slope of about 1.4, for all concentrations considered. The difference in cluster growth between the lower and higher concentration regimes can be understood by considering the number of free vacancies in the system. Figure 9 shows that, at higher concentrations, a greater fraction of vacancies is likely to be trapped in clusters. Section III A demonstrated that clusters have longer lifetimes, on average, at 900 K than at higher temperatures, so the growth of clusters at higher concentrations is most likely due to the
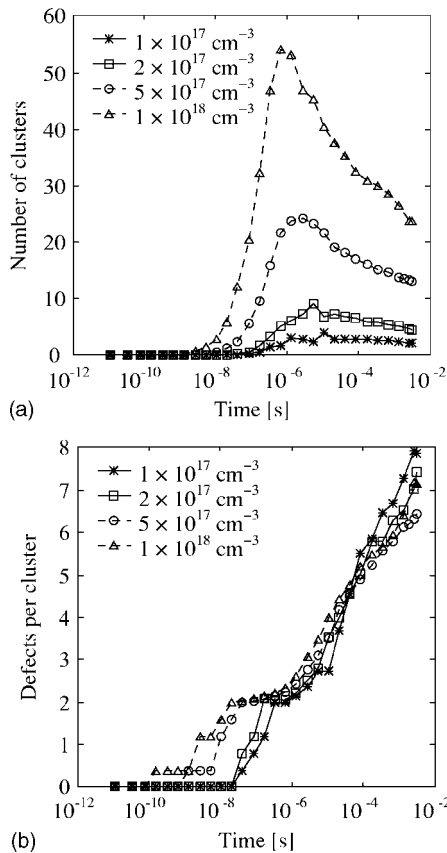

(a)

(b)

FIG. 8. Number of clusters (a) and cluster size (b) at various concentrations, with 18 shell interactions at 900 K.
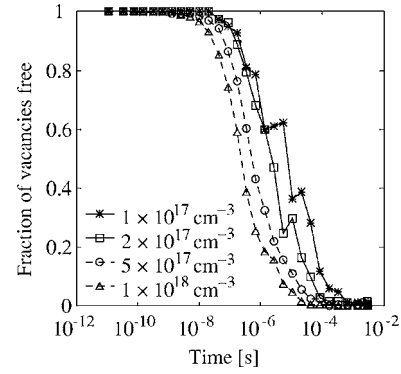

FIG. 9. Fraction of vacancies free at various concentrations, with 18 shell interactions at 900 K.

aggregation of smaller clusters, while at lower concentrations, the number of clusters stays relatively constant while the mean size increases and the number of free vacancies decreases. This implies that the capture of free vacancies drives cluster growth at lower concentrations. As with the temperature effects in Sec. III A, a cluster growth model which assumes either the aggregation or dissolution of small clusters across all concentrations will not accurately account for free vacancies in the system.

C. Interaction range

The simulations presented in this section were performed with a vacancy concentration of 10^{18} cm^{-3}, in a box of 102 of unit cells in each dimension, at 900 K. The interaction range varied from 4 to 18 lattice shells, using truncated and shifted forms of the vacancy pair interaction shown in Fig. 1. Figure 10 shows the vacancy diffusivity over time. Initially vacancies diffuse freely for all interaction ranges considered. As clusters form, the diffusivity decreases. The decrease is not as pronounced for the longest interaction range considered, 18 shells, at which the power law exponent $\gamma = -0.8$, as at the shorter interaction ranges, where the exponent $\gamma = 1.15 \pm 0.15$. This difference in γ leads, at long times, to a diffusivity which is roughly two orders of magnitude greater, with 18 shell interactions, than the diffusivity calculated with shorter range interactions. The number of clusters and cluster size, shown in Figs. 11(a) and 11(b), respectively, show a
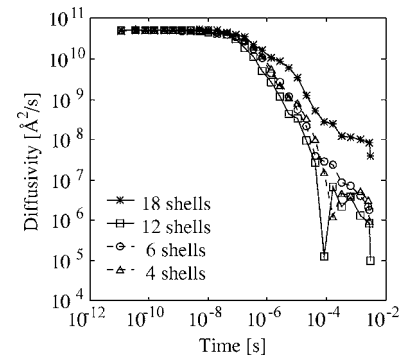

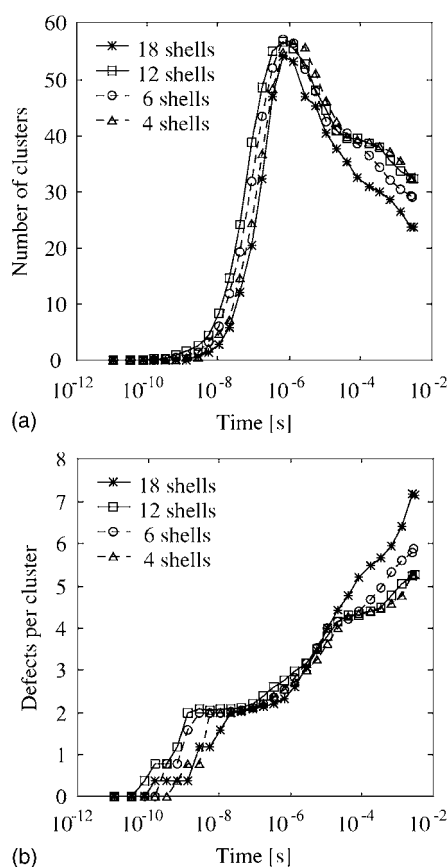FIG. 10. Vacancy diffusivity at various interaction ranges, with 10^{18} V cm^{-3} at 900 K.

FIG. 11. Number of clusters (a) and cluster size (b) at various interaction ranges, with 10^{18} V cm^{-3} at 900 K.

FIG. 12. Fraction of vacancies free at various interaction ranges, with 10^{18} V cm^{-3} at 900 K.

slight difference in long and short range interactions. The longest range interactions tend toward slightly larger, fewer clusters. Figure 12 shows the fraction of vacancies free, which is similar over time for the interaction ranges considered. From these trends, a large interaction range leads to greater vacancy diffusivity over time, which produces fewer clusters.

IV. CONCLUSIONS

We have presented results of kinetic lattice Monte Carlo simulations using long range interactions, to the 18th nearest lattice neighbor, and large numbers of vacancies, simulated over relatively long time. We studied the vacancy clustering behavior as a function of temperature, concentration, and interaction range, visiting defects in random order at each simulation step. Higher tempera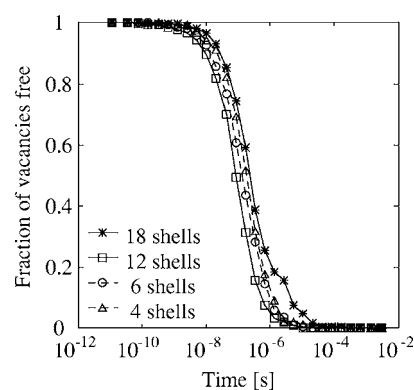tures led to fewer, but larger, vacancy clusters, which existed for shorter times, on average, than clusters formed at lower temperatures and which grew by attracting free vacancies. At lower temperatures, clusters grew by the dissociation and aggregation of smaller clusters. This difference in growth mechanism has not been reported or incorporated in any of the previously referenced models. For higher vacancy concentrations, more clusters formed than at lower concentrations, with fewer free vacancies, but the average size of the clusters did not depend on concentration. This result has not been previously reported. A longer interaction range led to a greater diffusivity with fewer clusters.

We have also demonstrated that vacancy diffusivities are time dependent, decreasing over time according, approximately, to a power law, $D(t) \sim t^{-\gamma}$. When the interaction range was long, 18 shells, γ increased with increasing concentration, keeping temperature constant, and decreased with increasing temperature at fixed concentration. Shorter interaction ranges led to greater values of γ. The number and size of vacancy clusters were also shown to depend on time, in addition to the temperature and concentration. None of the previously referenced models have explored these time dependences.

[1] M. D. Giles, S. Yu, H. W. Kennel, and P. A. Packan, *Defects and Diffusion in Silicon Processing* (Materials Research Society, Pittsburg, PA, 1997), Vol. 469, p. 253.

[2] D. J. Eaglesham, T. E. Haynes, H. J. Gossmann, D. C. Jacobson, P. A. Stolk, and J. M. Poate, Appl. Phys. Lett. **70**, 3281 (1997).

[3] V. C. Venezia, L. Pelaz, H.-J. L. Gossmann, T. E. Haynes, and C. S. Rafferty, Appl. Phys. Lett. **79**, 1273 (2001).

[4] A. Sultan, S. Banerjee, S. List, and V. McNeil, Appl. Phys. Lett. **83**, 8046 (1998).

[5] J. D. Ng, B. Lorber, J. Witz, A. Théobald-Dietrich, D. Kern, and

R. Giegé, J. Phys.: Condens. Matter **168**, 50 (1996).

[6] G. Madras and B. J. McCoy, J. Chem. Phys. **115**, 6699 (2001).

[7] A. Bongiorno and L. Colombo, Phys. Rev. B **57**, 8767 (1998).

[8] F. H. Stillinger and T. A. Weber, Phys. Rev. B **31**, 5262 (1985).

[9] T. E. M. Staab, A. Sieck, M. Haugk, M. J. Puska, T. Frauenheim, and H. S. Leipner, Phys. Rev. B **65**, 115210 (2002).

[10] A. La Magna, S. Coffa, and L. Colombo, Phys. Rev. Lett. **82**, 1720 (1999).

[11] S. Chakravarthi and S. T. Dunham, J. Appl. Phys. **89**, 4758 (2001).

[12] M. Prasad and T. Sinno, Phys. Rev. B **68**, 045206 (2003).

[13] M. Prasad and T. Sinno, Phys. Rev. B **68**, 045207 (2003).

[14] N. Metropolis, A. W. Rosenbluth, M. N. Rosenbluth, A. H. Teller, and E. Teller, J. Chem. Phys. **21**, 1087 (1953).

[15] M. Tang, L. Colombo, J. Zhu, and T. Diaz de la Rubia, Phys. Rev. B **55**, 14279 (1997).

[16] M. M. Bunea and S. T. Dunham, Phys. Rev. B **61**, R2397 (2000).

[17] M. M. Bunea and S. T. Dunham, *Defects and Diffusion in Silicon Processing* (Ref. 1), p. 353.

[18] G. Kresse and J. Furthmüller, Phys. Rev. B **54**, 11169 (1996).

[19] H. J. Monkhorst and J. D. Pack, Phys. Rev. B **13**, 5188 (1976).